

# VERA Status Report

Mizusawa VLBI Observatory,  
National Astronomical Observatory of Japan

21 September, 2016

## Contents

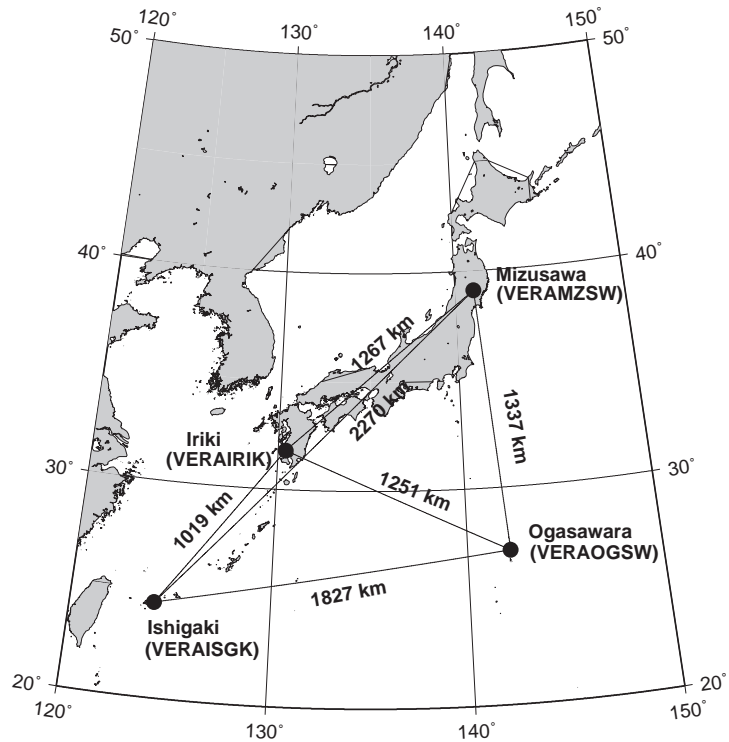
<b>1</b>	<b>Introduction</b>	<b>2</b>
<b>2</b>	<b>System</b>	<b>2</b>
2.1	Array . . . . .	3
2.2	Antennas . . . . .	4
2.2.1	Aperture Efficiency . . . . .	5
2.2.2	Beam Pattern and Size . . . . .	8
2.2.3	Pointing Accuracy . . . . .	9
2.2.4	Sky Line . . . . .	12
2.3	Receivers . . . . .	13
2.4	Digital signal process . . . . .	14
2.5	Recorders . . . . .	17
2.6	Correlators . . . . .	17
2.7	Calibration . . . . .	17
2.7.1	Delay and Bandpass Calibration . . . . .	17
2.7.2	Gain Calibration . . . . .	19
2.7.3	Phase Calibration . . . . .	19
2.8	C-band Information . . . . .	19
2.9	Geodetic Measurement . . . . .	19
<b>3</b>	<b>Observing Proposal</b>	<b>21</b>
3.1	Proposal Submission . . . . .	21
3.2	Observation Mode . . . . .	21
3.3	Angular Resolution . . . . .	21
3.4	Sensitivity . . . . .	22

3.5	Astrometric Observation . . . . .	23
3.6	Calibrator Information . . . . .	23
3.7	Nobeyama 45-m and Kashima 34-m Telescopes . . . . .	23
3.8	Date Archive . . . . .	24
<b>4</b>	<b>Observation and Data Reduction</b>	<b>26</b>
4.1	Preparation . . . . .	26
4.2	Observation and correlation . . . . .	26
4.3	Data Reduction . . . . .	26
4.4	Further Information . . . . .	27

# 1 Introduction

This document summarizes the current observational capabilities of VERA (VLBI Exploration of Radio Astrometry), which is operated by National Astronomical Observatory of Japan (NAOJ). VERA is a Japanese VLBI array to explore the 3-dimensional structure of the Milky Way Galaxy based on high-precision astrometry of Galactic maser sources. VERA array consists of four stations located at Mizusawa, Iriki, Ogasawara, and Ishigaki-jima with baseline ranges from 1000 km to 2300 km (see, figure 1). The construction of VERA array was completed in 2002, and it is under regular operation since the fall of 2003. VERA was opened to international users in the 22 GHz band (K band) and the 43 GHz band (Q band) from 2009. And also, VERA was opened in the 6.7 GHz band (C band) as a shared-risk observation from 2011. This document is intended to give astronomers necessary information for proposing observations with VERA.

Figure 1: Array configuration of VERA.



## 2 System

Most unique aspect of VERA is "dual-beam" telescope, which can simultaneously observe nearby two sources. While single-beam VLBI significantly suffers from fluctuation of atmosphere, dual-beam observations with VERA effectively cancel out the atmospheric fluctuations, and then VERA can measure relative positions of target sources to reference sources with higher accuracy based on the 'phase-referencing' technique.

## 2.1 Array

VERA array consists of 4 antenna site in Mizusawa, Iriki, Ogasawara, and Ishigaki-jima, with 6 baselines (see, figure 1). The maximum baseline length is 2270-km between Mizusawa and Ishigaki-jima, and the minimum baseline length is 1019-km between Iriki and Ishigaki-jima. The maximum angular resolution expected from the baseline length is about 1.2 mas for K band (22 GHz) and about 0.6 mas for Q band (43 GHz). The geographic locations of each VERA antenna in the coordinate system of epoch 2009.0 are summarized in table 1. Figures 2 show examples of  $uv$  plane coverage.

The coordinates and averaged velocities of VERA sites in Table 1 are predicted value at the epoch of January 01, 2015. Reference frame of these coordinates is ITRF2008. The rates of the coordinates of Mizusawa, Iriki, Ogasawara and Ishigaki-jima are the average value of change of the coordinates from January 01, 2014 to December 31, 2014. The 2011 off the Pacific coast of Tohoku Earthquake (Mj=9.0) brought the co-seismic large step and non-linear post-seismic movement to the coordinates of Mizusawa. Co-seismic steps of the coordinates of Mizusawa are  $dX=-2.0297\text{m}$ ,  $dY=-1.4111\text{m}$  and  $dZ=-1.0758\text{m}$ . The creeping continues still now, though decreased. The changes of coordinates by the post-seismic creeping are  $dX=-0.8574\text{m}$ ,  $dY=-0.5387\text{m}$  and  $dZ=-0.2398\text{m}$  in total from March, 12, 2011 to Jan, 01, 2015.

Table 1: Geographic locations and motions of each VERA antenna

Site	East Longitude [° ' '' ]	North Latitude [° ' '' ]	Ellipsoidal Height [m]	Altitude [m]
Mizusawa	141 07 57.31	39 08 00.68	116.4	75.6
Iriki	130 26 23.60	31 44 52.43	573.6	541.6
Ogasawara	142 12 59.80	27 05 30.49	273.1	222.9
Ishigaki	124 10 15.59	24 24 43.82	65.1	38.5

Site	X (m)	Y (m)	Z (m)	IVS2 <sup>a</sup>	IVS8 <sup>b</sup>	CDP <sup>c</sup>
Mizusawa	-3857244.6475	3108782.9982	4003899.2132	Vm	VERAMZSW	7362
Iriki	-3521719.8292	4132174.6212	3336994.1399	Vr	VERAIRIK	7364
Ogasawara	-4491068.5584	3481545.0777	2887399.7419	Vo	VERAOGSW	7363
Ishigaki	-3263995.1630	4808056.3180	2619948.7989	Vs	VERAISGK	7365

<sup>a</sup>IVS 2-characters code, <sup>b</sup>IVS 8-characters code, <sup>c</sup>CDP (NASA Crustal Dynamics Project) code

Site	$\Delta X$ (m/yr)	$\Delta Y$ (m/yr)	$\Delta Z$ (m/yr)
Mizusawa	-0.1108	-0.0471	-0.0050
Iriki	-0.0223	-0.0101	-0.0131
Ogasawara	0.0273	0.0261	0.0126
Ishigaki	-0.0411	-0.0014	-0.0476

The epoch of the coordinates is January, 01, 2015

Average speed was obtained from the VLBI data from January 01, 2014 to June 10, 2016.

Post seismic movements of Mizusawa are very complex. Internal error of coordinates of Mizusawa by polynomial fitting is 5-6mm. But, in a solution, a several centimeters differences arise for every fitting with the increase in geodetic observation data. It is judged that these differences are the uncertainly of the coordinates of Mizusawa.

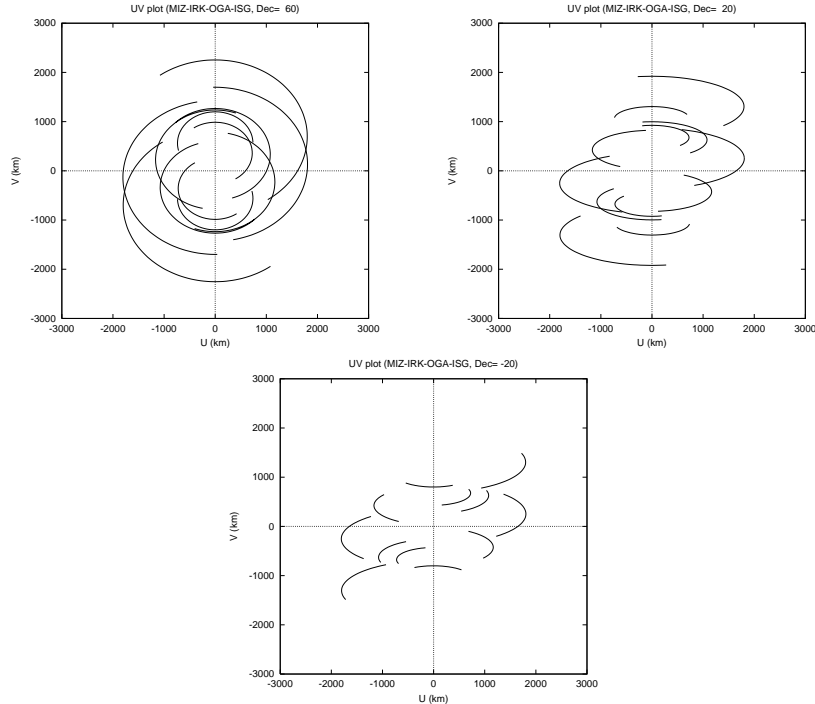


Figure 2:  $UV$  coverage ( $\pm 3000$  km) expected with VERA four antennas from an observation over elevation of  $20^\circ$ . Each panel show  $UV$  coverage for the declination of  $60^\circ$  (top left),  $20^\circ$  (top right), and  $-20^\circ$  (bottom).

## 2.2 Antennas

All the telescopes of VERA have the same design, being a Cassegrain-type antenna on AZ-EL mount. Each telescope has a 20-m diameter dish with a focal length of 6-m, with a sub-reflector of 2.6-m diameter. The dual-beam receiver systems for 22 and 43 GHz are installed at the Cassegrain focus. Two receivers are set up on the Stewart-mount platforms, which are sustained by steerable six arms, and with such systems one can simultaneously observe two adjacent objects with a separation angle between 0.32 and 2.2 (2.18 for 43 GHz) deg. The whole receiver systems are set up on the field rotator (FR), and the FR rotate to track the apparent motion of objects due to the earth rotation. Table 2 summarizes the ranges of elevation (EL), azimuth (AZ) and field rotator angle (FR) with their driving speeds and accelerations. The examples of duration time which requires to set a separation angle between two receiver on the Stewart-mount platforms are summarized in table 3. In the case of single beam observing mode, one of two beams is placed at the antenna vertex (separation offset of 0 deg).

Table 2: Driving Performance of VERA 20-m Antennas

Driving axis	Driving range	Max. driving speed	Max. driving acceleration
AZ <sup>1</sup>	$-90^\circ \sim 450^\circ$	$2.1^\circ/\text{sec}$	$2.1^\circ/\text{sec}^2$
EL	$5^\circ \sim 85^\circ$	$2.1^\circ/\text{sec}$	$2.1^\circ/\text{sec}^2$
FR <sup>2</sup>	$-270^\circ \sim 270^\circ$	$3.1^\circ/\text{sec}$	$3.1^\circ/\text{sec}^2$

<sup>1</sup>The north is  $0^\circ$  and the east is  $90^\circ$ .

<sup>2</sup>FR is  $0^\circ$  when Beam-1 is at the sky side and Beam-2 is at the ground side, and CW is positive when an antenna is seen from a target source.

Table 3: Moving Time of Two Receiver System

Starting separation	End separation	Duration time
0.32°	0.5°	11 sec
0.32°	1.0°	30 sec
0.32°	1.5°	55 sec
0.32°	2.0°	86 sec
0.32°	2.2°	98 sec

### 2.2.1 Aperture Efficiency

The aperture efficiency of each VERA antenna is about 45–50% in the K-band and about 35–50% in the Q-band. (see table 4 and figure 3). These measurements were based on the observations of Jupiter assuming that the brightness temperature of Jupiter is 160 K in both the K band and the Q band. The latest measurements were done in 2016 February. The aperture efficiencies are not significantly changed compared with previous measurements. The measurement results will be revised in the next winter season.

Table 4: The Latest Results of Aperture Efficiency Measurements of the VERA 20 m Antennas

Site	Band	Date	$\eta_A$ (%)	HPBW (arcsec)	Num. of Scans	Elevation (deg)	$\theta^b$ (arcsec)
MIZ	Q	Feb. 6, 2016	47.3±1.6	72.8±9.6	25	47-55	41.6
IRK	Q	Dec. 8, 2015	40.3±2.1	74.6±4.7	16	52-62	35.1
	Q	Feb. 8, 2016	41.8±1.3	76.8±8.7	9	46-61	41.6
OGA	Q	Feb. 8, 2016	38.3±3.8	84.8±10.5	5	57-67	41.6
	Q	Feb. 10, 2016	41.3±3.5	78.2±13.5	16	59-68	41.6
ISG	Q	Dec. 25, 2015	45.9±4.8	77.5±11.8	7	56-69	35.1
	Q	Feb. 6, 2016	44.0±2.2	77.4±4.7	9	43-63	41.6
MIZ	K	Feb. 7, 2016	44.7±4.1	152.3±21.7	10	48-55	41.6
	K	Feb. 10, 2016	50.9±4.5	144.7±5.4	6	49-55	41.6
	K	Feb. 18, 2016	47.8±0.6	143.1±5.3	14	53-55	42.7
IRK	K	Dec. 7, 2015	45.5±0.7	143.8±6.1	12	57-63	35.1
	K	Feb. 10, 2016	47.0±0.6	139.7±6.4	15	48-62	41.6
OGA	K	Feb. 7, 2016	45.9±0.4	142.4±7.3	13	56-67	41.6
ISG	K	Feb. 7, 2016	47.5±2.5	143.5±10.6	11	43-64	41.6

<sup>a</sup> Assumed apparent diameter for Jupiter.

The elevation dependence of aperture efficiency for VERA antenna was also measured from the observation toward maser sources. Figure 4 show the relations between the elevation and the aperture efficiency measured for Iriki station. The aperture efficiency in low elevation of  $\leq 20$  deg decreases slightly, but this decrease is less than about 10%. Concerning this elevation dependence, the observing data FITS file include a gain curve table (GC table), which is AIPS readable, in order to calibrate the dependence when the data reduction.

The aperture efficiency was also measured at various separation angle of dual-beams in order to evaluate the dependence of aperture efficiency on dual-beam separation angle. Figure 5 show the relations between the beam separation angle and the aperture efficiency measured for Iriki antenna. It appears that the aperture efficiency decreases slightly as the separation angle increases. For the calibration of the separation angle dependence, a gain curve table (GC table) which includes the separation angle

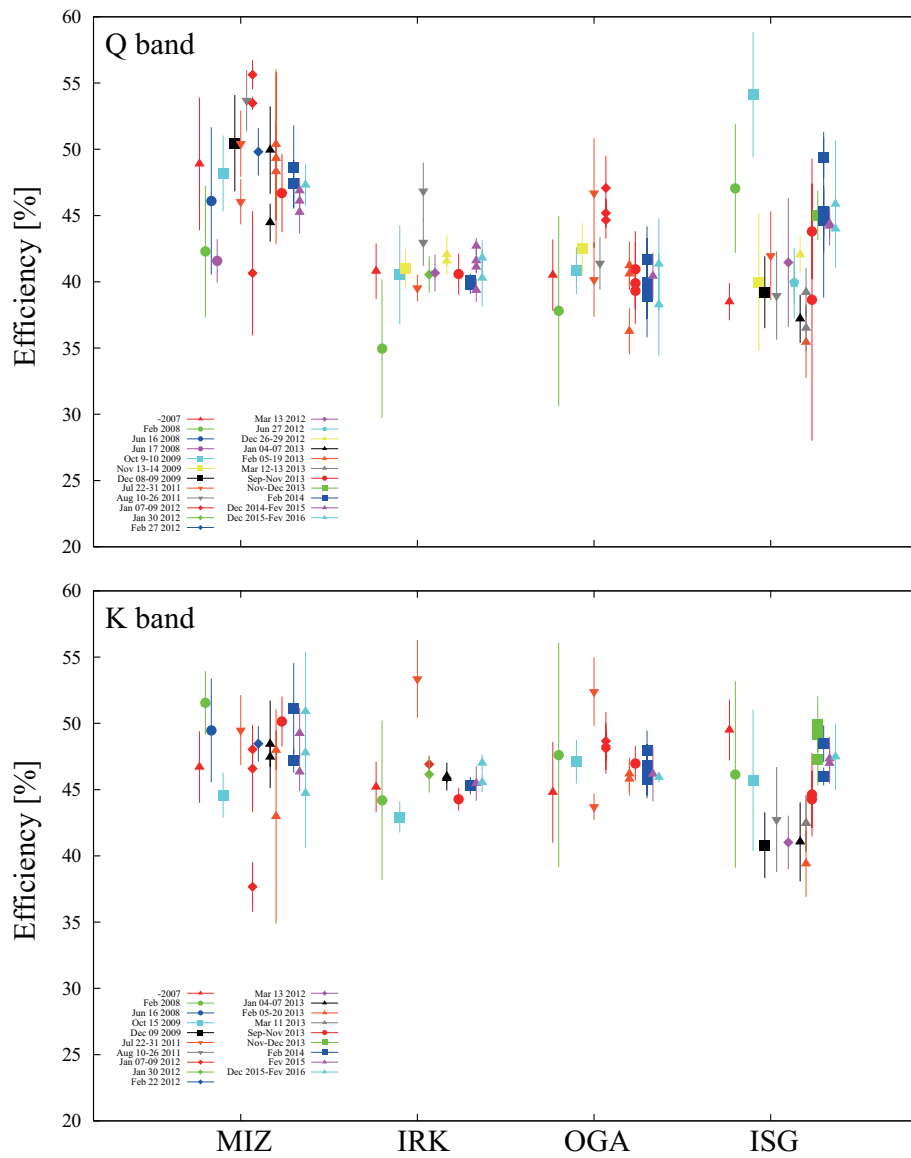


Figure 3: History of the aperture efficiency measurements for the VERA antennas.

dependence of the aperture efficiency is attached to the observed data FITS file.

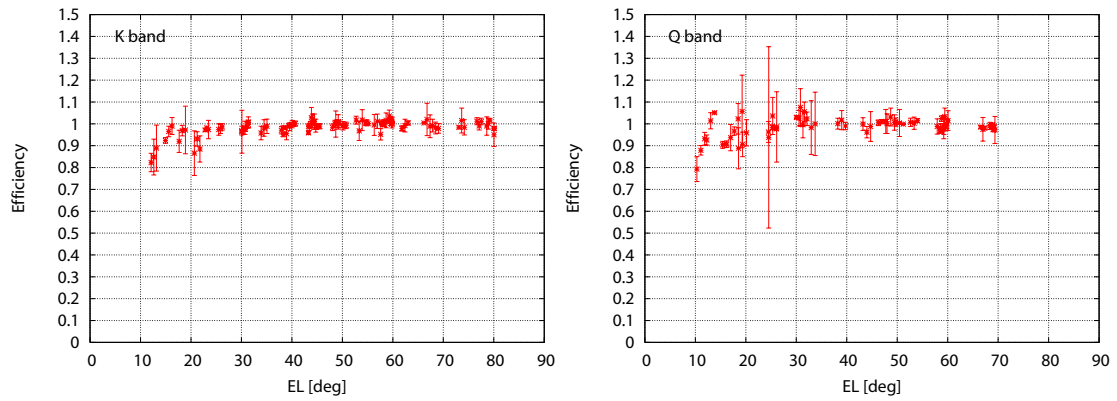


Figure 4: The elevation dependence of the aperture efficiency in the K band (on Feb 8, 2005; *right*) and the Q band (on Feb 12, 2005; *left*) for Iriki antenna. The efficiency is relative value to the measurement at  $EL = 50^\circ$ .

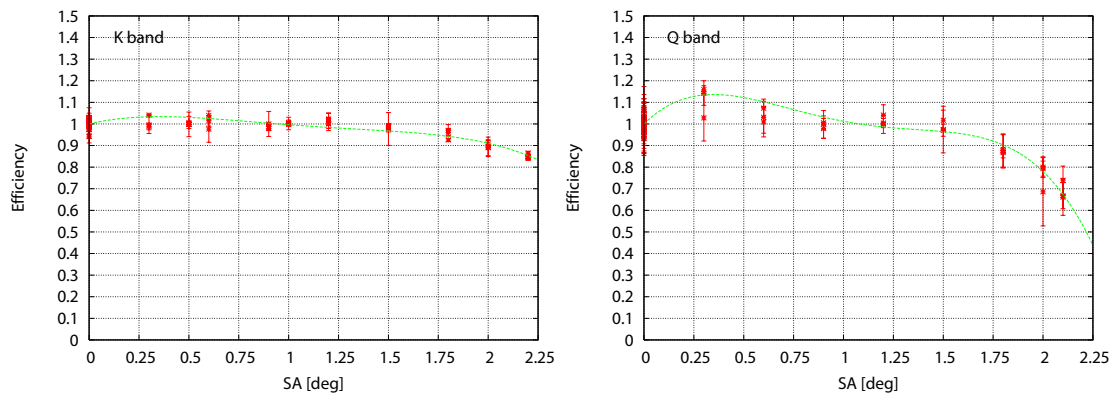


Figure 5: The dependence of the aperture efficiency on the separation angle between dual-beams in the K band (on Mar 4, 2004; *right*) and the Q band (on Mar 5, 2004; *left*) for Iriki antenna. The efficiency of vertical axis is relative value to the measurement at the separation angle of  $0^\circ$ . The curved line indicates the quartic polynomial fitting.



## 2.2.2 Beam Pattern and Size

Figure 6 show the beam patterns in the K band. The side-lobe level is less than about  $-15$  dB, except for the relatively high side-lobe level of about  $-10$  dB for the separation angle of  $2.0$  deg at Ogasawara station. The side-lobe of the beam patterns have an asymmetric shape, but the main beam have a symmetric Gaussian shape without dependence on separation angle. The measured beam sizes (HPBW) in the K band and the Q band based on the data of the pointing calibration are also summarized in table 4. The main beam sizes show no dependence on the dual-beam separation angle.

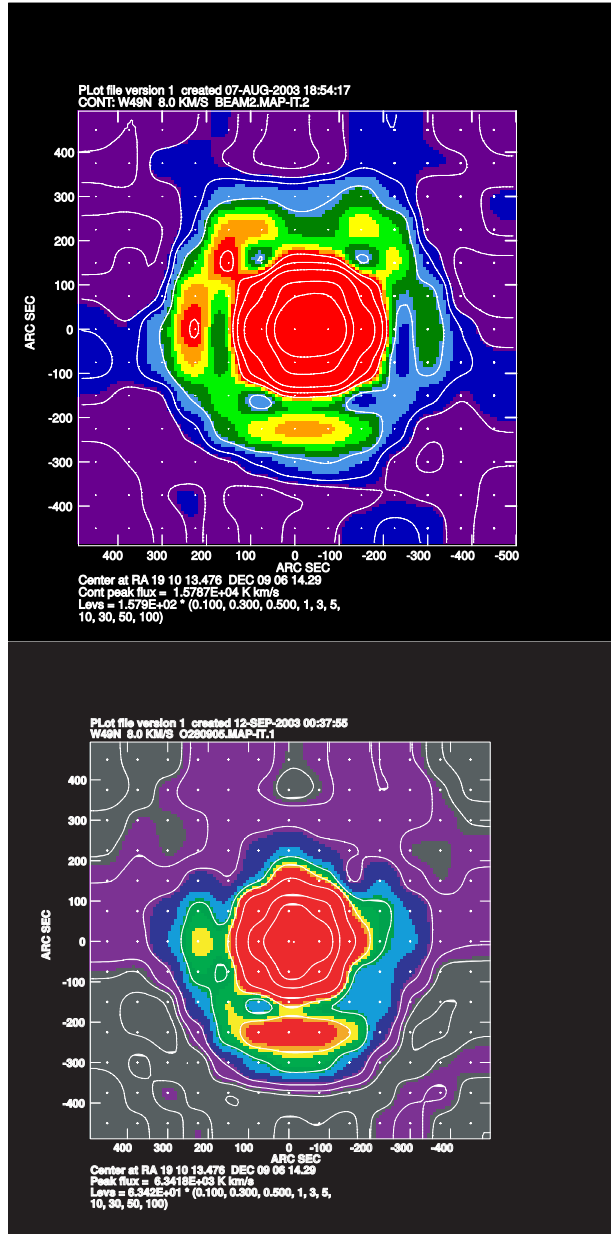


Figure 6: The beam patterns of Beam-A in the K band. Top and bottom panels were the results for the separation angle of  $0^\circ$  at Iriki, and for the separation angle of  $2.0^\circ$  at Ogasawara, respectively. These are derived from the mapping observation of strong  $H_2O$  maser toward W49N, which can be assumed as a point source, with grid spacing of  $75''$ .

### 2.2.3 Pointing Accuracy

In each VERA antenna, observations to check a pointing accuracy were carried out, and the pointing offset were calibrated. Pointing offsets for all sky direction were measured based on five-point scans in the azimuth and elevation direction using strong maser sources with known positions. Observed pointing offsets were parameterized with the models described in the equation (1) and (2), and are now corrected to improve the pointing accuracy. In the equations (1) and (2),  $A_1$ - $A_8$  are standard pointing instrumental parameters for AZ-EL mounting telescope, and  $A_9$ - $A_{12}$  are parameters which are introduced to describe higher order effects.

$$\begin{aligned} \delta Az &= A_1 \sin(Az) \sin(El) - A_2 \cos(Az) \sin(El) + A_3 \sin(El) + A_4 \cos(El) + A_5 + \\ &A_9 \sin(2Az) \sin(El) - A_{10} \cos(2Az) \sin(El) + \\ &A_{11} \sin(2Az) \cos(El) - A_{12} \cos(2Az) \cos(El) \end{aligned} \quad (1)$$

$$\begin{aligned} \delta El &= A_1 \cos(Az) + A_2 \sin(Az) + A_6 + A_7 \cos(El) + A_8 \sin(El) + \\ &A_9 \cos(2Az) - A_{10} \sin(2Az) \end{aligned} \quad (2)$$

The pointing accuracy of each VERA antenna, after the correction of the pointing instrumental error, are summarized in the table 5. Figure 7 shows examples of the residual pointing offsets in the Q band.

Table 5: Pointing Accuracy of VERA 20-m Antennas

Site	Band	Date	$\sigma_{AZ}$ (arcsec)	$\sigma_{EL}$ (arcsec)	Num. of Scan
MIZ	Q	Jul. 22 2016	5.340	5.500	198
IRK	Q	Aug. 02 2016	6.176	7.450	162
OGA	Q	Aug. 12 2016	5.308	7.969	178
ISG	Q	Jul. 21 2016	6.635	7.886	195

Note;  $\sigma_{AZ}$  and  $\sigma_{EL}$  represent the standard deviation of the pointing measurements in AZ and EL, respectively.

The pointing measurements were carried out only in the Q band.

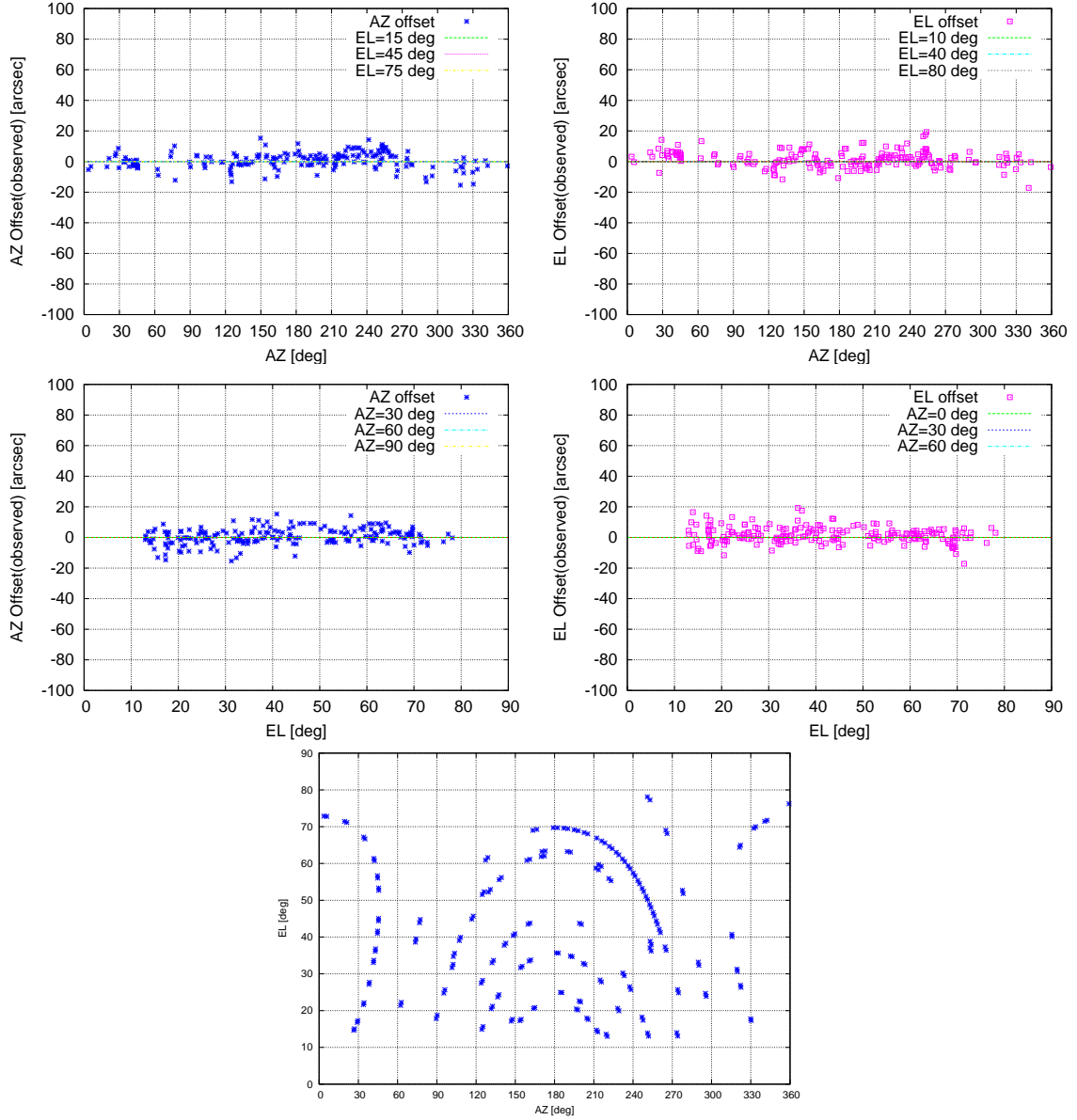


Figure 7: Examples of pointing residuals for the Mizusawa antenna in the Q band (43 GHz). Top and middle panels show relations of the azimuth and elevation, respectively, with the pointing residuals in azimuth (*left*) and elevation (*right*). Bottom panel shows positions on celestial sphere of the objects which were observed in the pointing measurement.

For dual-beam observations with large separation angle, there is an additional pointing offset with  $\sim 15$  arcsec that shows sinusoidal variations with FR angle, as shown in figure 8. This pointing error is not fully calibrated.

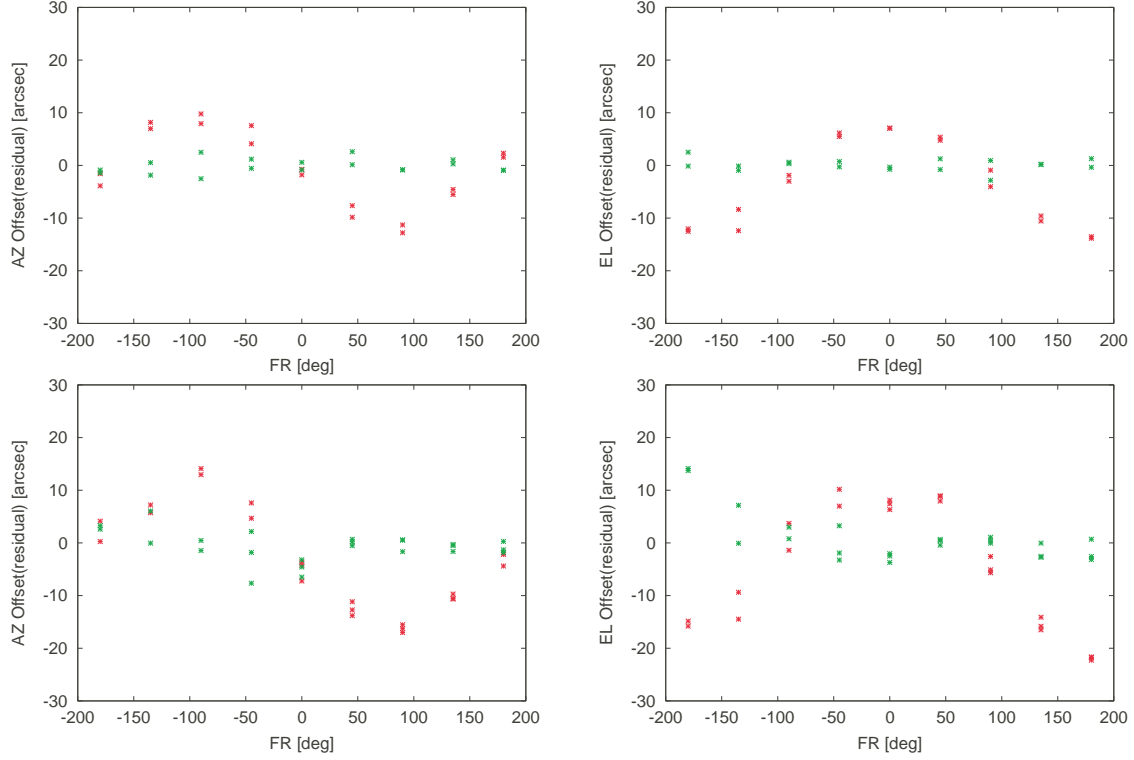


Figure 8: Pointing offset of Beam-A against dual-beam separation angle in the K band at Iriki station. Red cross indicate the tracking error with the dual-beam offset, and green cross indicate the tracking error without the dual-beam offset (Beam-A is placed at the antenna vertex). These panels show dependency on the field rotator angle (FR) of the azimuth offset (*left panel*) and the elevation offset (*right panel*). Top and bottom panels show the relations for the separation angle of 1.0 deg (on the observation of W3OH) and 2.0 deg (on the observation of W49N), respectively.

## 2.2.4 Sky Line

Figure 9 show a skyline for the VERA antenna site. While mechanically-possible EL driving range is from 5 to 85 deg, due to the sky line effect, the lowest observable elevation is as high as 20 deg depending on the stations and the directions. Observers are requested to take care of the skyline effect if low declination sources are to be observed.

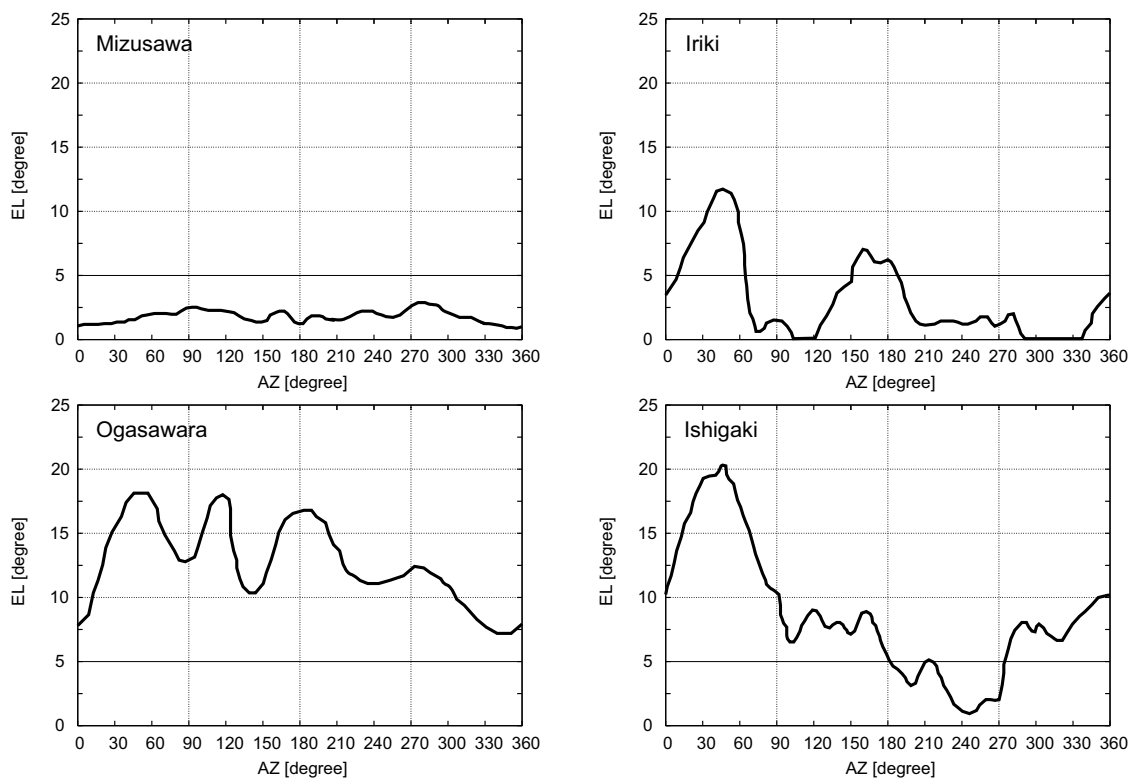


Figure 9: Sky Line for each VERA antenna. The azimuth of 0 deg is the north. Mechanically-possible EL range is from 5 deg to 85 deg.

## 2.3 Receivers

Each VERA antenna has the receivers for 5 bands, which are S, C, X, K, and Q bands. For the common use in 2017B, the K band (22 GHz), the Q band (43 GHz) and the C band (6.7 GHz) are open for observing. The information about the C band is described in session 2.8. The low-noise HEMT amplifiers in the K and Q bands are enclosed in the cryogenic dewar, which is cooled down to 20 K, to reduce the thermal noise. The range of observable frequency and the typical receiver noise temperature ( $T_{RX}$ ) at each band are summarized in the table 6 and figure 10.

Table 6: Receivers

Band	Frequency Range [GHz]	$T_{RX}^a$ [K]	Polarization
K	21.5-23.8	30-50	LCP
Q	42.5-44.5	40-60 <sup>b</sup> ,70-90 <sup>c</sup>	LCP

<sup>a</sup>Receiver noise temperature

<sup>b</sup>Receiver noise temperature for beam-A receiver

<sup>c</sup>Receiver noise temperature for beam-B receiver

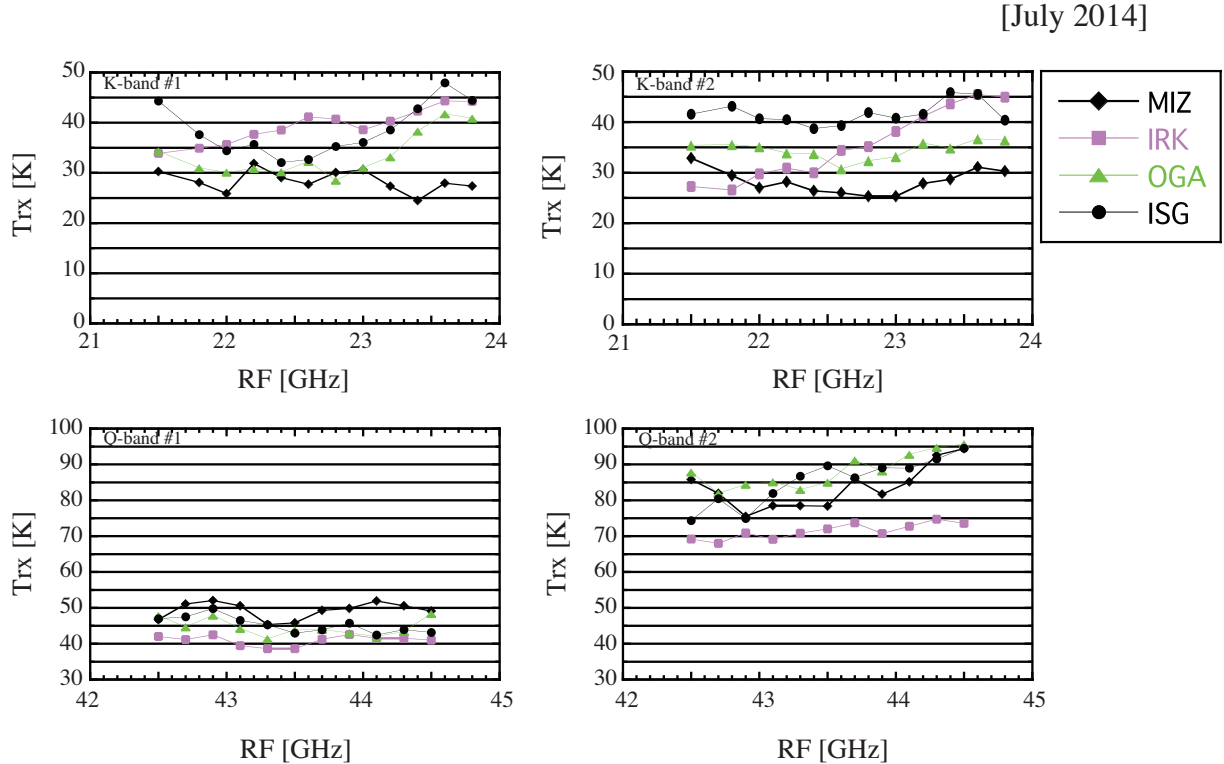


Figure 10: Receiver noise temperature for each VERA antenna. Top and bottom panels show measurements in the K and Q bands, and left and right panels show those in the receiver #1 for beam-A and #2 for beam-B, respectively. Horizontal axis indicate a RF (radio frequency) at which  $T_{RX}$  is measured.

After the radio frequency (RF) signals from astronomical objects are amplified by the receivers, the RF signals are mixed with standard frequency signal generated in the first local oscillator to down-convert the RF to an intermediate frequency (IF) of 4.7 GHz–7 GHz. The first local frequencies are fixed at 16.8 GHz in the K band and

at 37.5 GHz in the Q band. The IF signals are then mixed down again to the base band frequency of 0–512 MHz. The frequency of second local oscillator is tunable with a possible frequency range between 4 GHz and 7 GHz. The correction of the Doppler effect due to the earth rotation is carried out in the correlation process after the observation. Therefore, basically the second local oscillator frequency is kept to be constant during the observation. Figure 11 shows a flow diagram of these signals for the VERA.

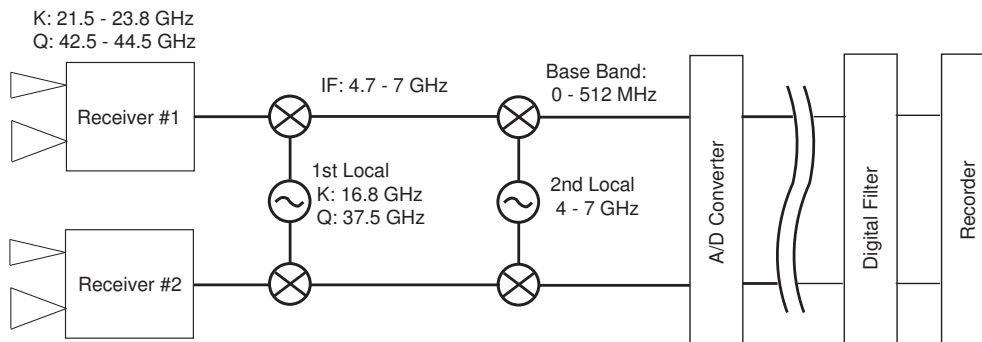


Figure 11: Flow diagram of signals from receiver to recorder for VERA.

## 2.4 Digital signal process

A/D (analog-digital) samplers convert the analog base band outputs (0–512 MHz  $\times$  2 beams) to digital form. The A/D converters carry out the digitization of 2-bit sampling with the bandwidth of 512 MHz and the data rate is 2048 Mbps for each beam.

Since the total data recording rate is limited to 1024 Mbps (see the next section), only part of the sampled data can be recorded onto hard disks. The data rate reduction is done by digital filter system, with which one can flexibly choose number and width of recording frequency bands. Observers can select modes of the digital filter listed in the table 7 and table 8. In VERA7Q mode in the table 7, two transitions ( $v=1$  & 2) of SiO maser in the Q band with the beam-A can be simultaneously recorded. VERA7C and VERA4S are modes for single-beam observations, such as C-band or imaging of continuum sources, etc.

Table 7: Digital Filter Mode for VERA

Mode	Rate (Mbps)	Num. CH <sup>a</sup>	BW/CH <sup>b</sup> (MHz)	CH <sup>c</sup>	Beam	Freq. range <sup>d</sup> (MHz)	Side Band <sup>e</sup>
VERA1	1024	2	128	1	A	256 - 384	U
				2	B	256 - 384	U
VERA1S	1024	2	128	1	A	128 - 256	L
				2	A	256 - 384	U
VERA7	1024	16	16	1	A	256 - 272	U
				2	B	128 - 144	U
				3	B	144 - 160	L
				4	B	160 - 176	U
				5	B	176 - 192	L
				6	B	192 - 208	U
				7	B	208 - 224	L
				8	B	224 - 240	U
				9	B	240 - 256	L
				10	B	256 - 272	U
				11	B	272 - 288	L
				12	B	288 - 304	U
				13	B	304 - 320	L
				14	B	320 - 336	U
				15	B	336 - 352	L
				16	B	352 - 368	U
VERA10	1024	16	16	1	A	256 - 272	U
				2	B	256 - 272	U
				3	A	272 - 288	L
				4	B	272 - 288	L
				5	A	288 - 304	U
				6	B	288 - 304	U
				7	A	304 - 320	L
				8	B	304 - 320	L
				9	A	320 - 336	U
				10	B	320 - 336	U
				11	A	336 - 352	L
				12	B	336 - 352	L
				13	A	352 - 368	U
				14	B	352 - 368	U
				15	A	368 - 384	L
				16	B	368 - 384	L

<sup>a</sup>Total number of channels<sup>b</sup>Bandwidth per channel in MHz<sup>c</sup>Channel number<sup>d</sup>Filtered frequency range in the base band (MHz)<sup>e</sup>Side Band (LSB/USB)



Table 8: Digital Filter Mode for VERA : continued

Mode	Rate (Mbps)	Num. CH <sup>a</sup>	BW/CH <sup>b</sup> (MHz)	CH <sup>c</sup>	Beam	Freq. range <sup>d</sup> (MHz)	Side Band <sup>e</sup>
VERA7Q	1024	16	16	1	A	48 - 64	L
				2	B	48 - 64	L
				3	B	64 - 80	U
				4	B	96 - 112	U
				5	B	128 - 144	U
				6	B	160 - 176	U
				7	B	192 - 208	U
				8	B	224 - 240	U
				9	A	352 - 368	U
				10	B	256 - 272	U
				11	B	288 - 304	U
				12	B	320 - 336	U
				13	B	352 - 368	U
				14	B	384 - 400	U
				15	B	416 - 432	U
				16	B	448 - 464	U
VERA7C	1024	16	16	1	A	0 - 16	U
				2	A	32 - 48	U
				3	A	64 - 80	U
				4	A	96 - 112	U
				5	A	128 - 144	U
				6	A	160 - 176	U
				7	A	192 - 208	U
				8	A	224 - 240	U
				9	A	256 - 272	U
				10	A	288 - 304	U
				11	A	320 - 336	U
				12	A	352 - 368	U
				13	A	384 - 400	U
				14	A	416 - 432	U
				15	A	448 - 464	U
				16	A	480 - 496	U
VERA4S	1024	8	32	1	A	128 - 160	U
				2	A	160 - 192	L
				3	A	192 - 224	U
				4	A	224 - 256	L
				5	A	256 - 288	U
				6	A	288 - 320	L
				7	A	320 - 352	U
				8	A	352 - 384	L

<sup>a</sup>Total number of channels<sup>b</sup>Bandwidth per channel in MHz<sup>c</sup>Channel number<sup>d</sup>Filtered frequency range in the base band (MHz)<sup>e</sup>Side Band (LSB/USB)

## 2.5 Recorders

VERA is using a hard-disk recording system called OCTADISK which can record with the rate of 1 Gbps. However, in combined observations with Nobeyama 45-m and/or Kashima 34-m telescope, the data are recorded with the rate of 2 Gbps and only the data of one single beam are recorded.

## 2.6 Correlators

The correlation processes are carried out by the software correlator located at NAOJ Mizusawa campus. In a default correlation, the maximum number of spectral point per antenna are 2048 points across all channels of 2-beams data and the time resolution is usually set to be 1 second. But higher spectral resolution and higher time resolution are available by the software correlator upon requests. Please contact with vera-prop@nao.ac.jp, if you require correlating with special parameters.

## 2.7 Calibration

### 2.7.1 Delay and Bandpass Calibration

The time synchronization for each antenna is kept within 0.1  $\mu$ sec using GPS and high stability frequency standard provided by the hydrogen maser. To correct for clock parameter offsets with better accuracy, bright continuum sources with accurately-known positions should be observed at usually every 60–90 mins during observations. The calibration of frequency characteristic (bandpass calibration) can be also done based on the observation of bright continuum source.

The bandpass characters of the base band in frequency could cause some CH-to-CH amplitude offset in the visibility output depending on the digital filter mode. The frequency dependence of the visibility amplitude at K and Q bands are shown in figure 12 and 13. Differences of the dependence between 2011 and 2012 are less than 10%. External text files for GC tables are available to calibrate such CH-to-CH amplitude offsets for VERA7 mode at K and Q band, VERA7MM mode at K band, and VERA7SIO2 (same as VERA7Q) mode at Q band. This calibration is essential to treat each CH data independently as in the case of multi-CH mapping, or to obtain the accurate amplitude value from the visibility data across the all CHs. Please access to the website and download the calibration files in table 9. Then please import the calibration file using the AIPS task “TBIN”.

Table 9: Information for calibration of CH-to-CH amplitude offset

URL	in preparation, please ask "vera-prop @ nao.ac.jp"
File for VERA7	GCTAB_VERA7_K2009 GCTAB_VERA7_Q2009
File for VERA7MM	GCTAB_VERA7MM_K2009
File for VERA7SIO2	GCTAB_VERA7SIO2_Q2009

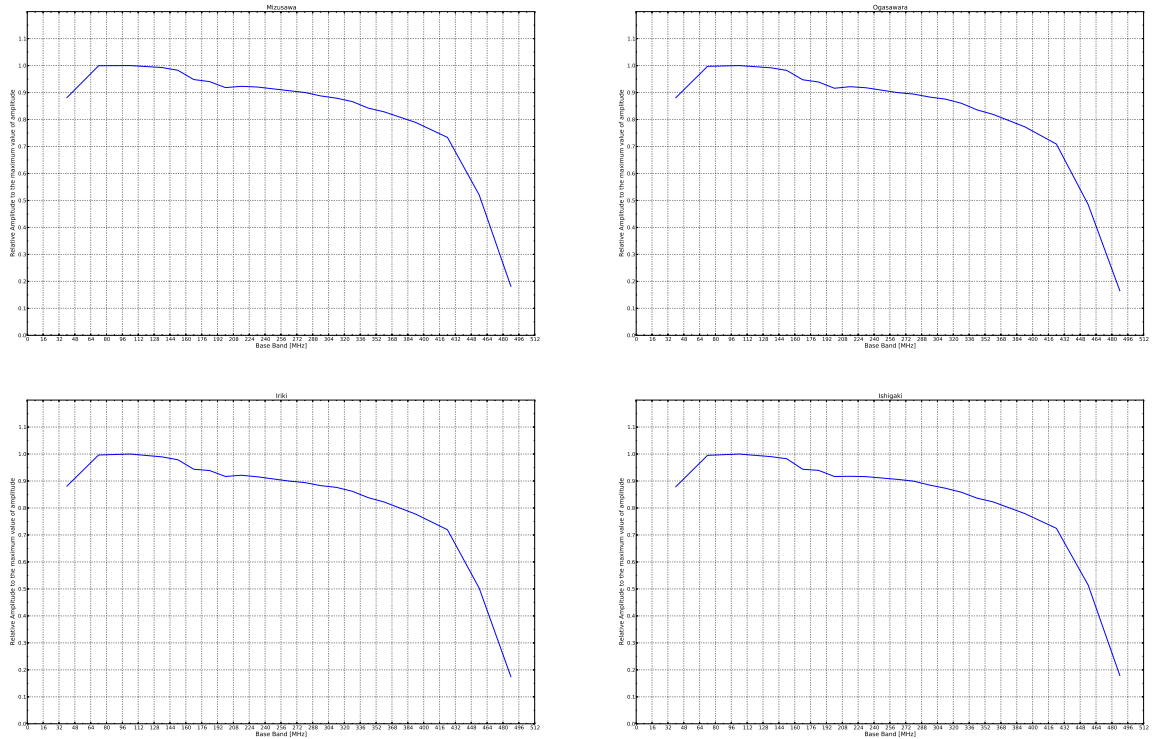


Figure 12: The frequency dependence of the baseband at K band seen for each VERA antenna; (*top-left*) Mizusawa, (*top-right*) Ogasawara, (*bottom-left*) Iriki, and (*bottom-right*) Ishigaki.

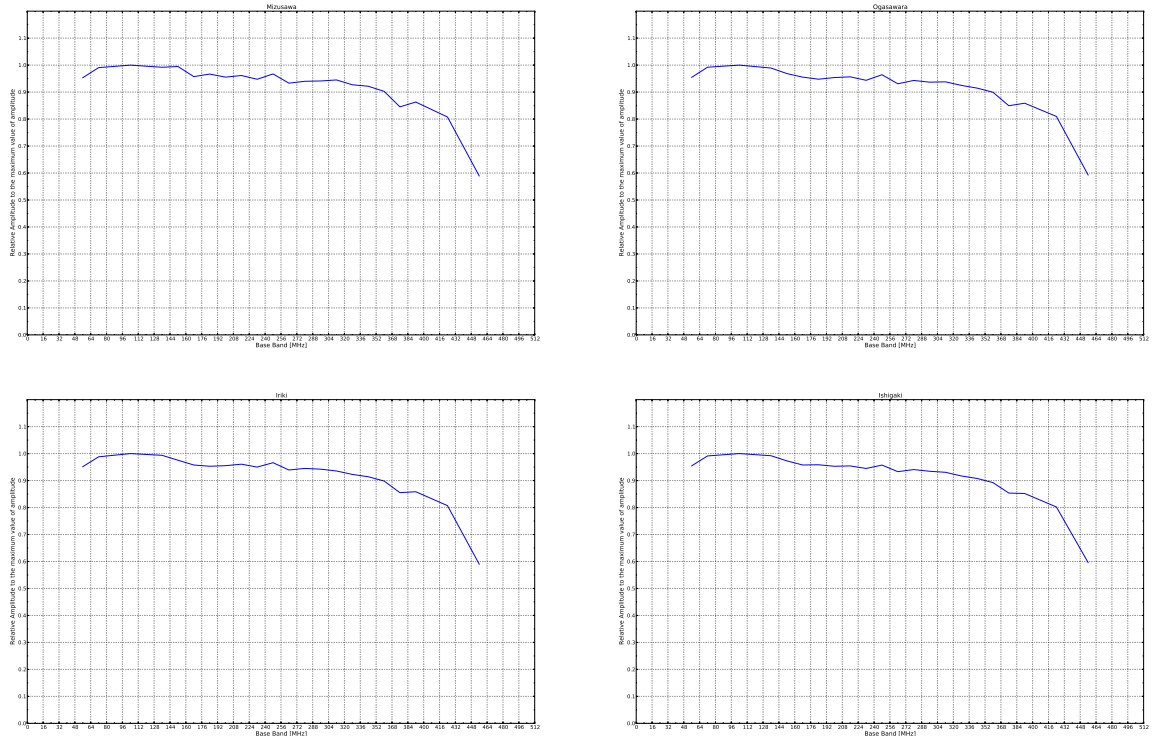


Figure 13: The frequency dependence of the baseband at Q band seen for each VERA antenna; (*top-left*) Mizusawa, (*top-right*) Ogasawara, (*bottom-left*) Iriki, and (*bottom-right*) Ishigaki.

### 2.7.2 Gain Calibration

Each VERA antenna has the chopper wheel of the hot load (black body at the room temperature), and the system noise temperature can be obtained by measuring the ratio of the sky power to the hot load power (so-called R-Sky method). The hot load measurement can be made before/after any scan. Also, the sky power is continuously monitored during scans, so that one can trace the variation of system noise temperature.

### 2.7.3 Phase Calibration

To calibrate the instrumental phase error by caused the path length difference in dual-beams, four artificial noise sources (NS) are installed on the feedome base (above the main reflector). During observations, the artificial noise (reflected by sub-reflector) is injected to dual-beam receivers and correlated on real-time to calculate the phase difference between dual-beams. Typical phase residuals of the dual-beam calibration system are 0.2 mm for using one NS and 0.12 mm for using four NSs. Dual-beam phase calibration data are also attached to the observed data in a readable format with AIPS.

## 2.8 C-band Information

Antenna efficiency at C-band was estimated to be 50-55 % depending on the stations. The frequency range of C-band receiver is 6.5 - 7.0 GHz. Typical system temperature is around 130 K toward the zenith, and optical depth is around 0.03-0.05 under relatively good conditions. Beam size at 6.6 GHz is around 9 arcmin, and the pointing at C band is expected to be sufficiently high, as pointing model is based on measurements using a shaper beam at 22 GHz. Different from the case of K-band and Q-band, VERA 20-m telescope has only one C-band receiver, therefore only a single-beam observation is available.

## 2.9 Geodetic Measurement

Geodetic observations are performed as part of the VERA project observations to derive accurate antenna coordinates. The geodetic VLBI observations for VERA are carried out in the S/X bands (2 GHz/8 GHz) and also in the K band (22 GHz). The S/X bands are used in the the international experiments called IVS-T2 and AOV. On the other hand, the K band is used in the VERA internal experiments. We obtain higher accuracy results in the K band compared with the S/X bands. The most up-to-date geodetic parameters are derived through geodetic analyses.

Non-linear post seismic movement of Mizusawa after the 2011 off the Pacific coast of Tohoku Earthquake continues. The position and velocity of Mizusawa is continuously monitored by VLBI and GPS. The coordinates in the table 1 are provisional and will be revised with accumulation of geodetic data by GPS and VLBI.

In order to maintain the antenna position accuracy, the VERA project has three kinds of geodetic observations. The first is participation in IVS session, T2 and AOV (Asia-Oceania VLBI), in order to link the VERA coordinates to the ITRF2008 (International Terrestrial Reference Frame 2008). Basically Mizusawa station participate in IVS session nearly every month. Based on the observations for ten years, the 3-

dimensional positions and velocities of Mizusawa station till March 09, 2011 is determined with accuracies of 7-9 mm and about 1 mm/yr in ITRF2008 coordinate system. But the uncertainty of several centimeters exists in the position on and after March 11, 2011. The second kind of geodetic observations is monitoring of baseline vectors between VERA stations by internal geodetic VLBI observations. Geodetic positions of VERA antennas relative to Mizusawa antenna are measured from geodetic VLBI observations every two weeks. From polygonal fitting of the ten-year geodetic results, the relative positions and velocities are obtained in the precisions of 1-2 mm and 0.8-1 mm/yr till March 09, 2011.

## 3 Observing Proposal

For this observing season (January 15th, 2017 to July 15th, 2017), the K and Q bands dual-beam mode are opened to international users. Also, the C band single-beam mode is opened tentatively in this season. Total observing time up to 200 hrs per year will be available for the common-use observing time. The observation with 6 elements array (VERA + Nobeyama 45-m and Kashima 34-m) is available for the K band and the observation with VERA + Nobeyama 45-m is available for the Q bands ( the Q-band observation with Kashima 34-m is not available in this season). The observing time of the combined array is 100 hrs per year at maximum.

### 3.1 Proposal Submission

Observing proposals for VERA are invited for the observing period from January 15th, 2017 to July 15th, 2017. The application deadline is on “**November 1st 2016**” for this season. Proposals will be reviewed by referees, and observing time is scheduled by the VERA Time Allocating Committee of the NAOJ on the basis of the scientific merits of the proposed research. As for the proposal submission, details can be found at the VERA homepage,

<http://veraserver.mtk.nao.ac.jp/restricted/index-e.html>.

Any questions on proposal submission should be sent to “[vera-prop @ nao.ac.jp](mailto:vera-prop@nao.ac.jp)”. If an applicant wants to have a collaborator from the VERA group member for extensive support, the VERA group can arrange the collaborator (after the acceptance of proposal).

### 3.2 Observation Mode

The K band (22 GHz) and the Q band (43 GHz) single/dual-beam mode, and the C-band single-beam mode are available. In addition to VERA four antennas, Nobeyama 45-m and Kashima 34-m are available for the K-band and Nobeyama 45-m is available for the Q band. Only a single-beam observation is available in the combined observation with Nobeyama 45-m and/or Kashima 34-m.

The recording rate of 1 Gbps is used in the observation carried out with only VERA. However, the combined observation with Nobeyama 45-m and/or Kashima 34-m is made by a 2-Gbps recording rate as a shared-risk observation.

### 3.3 Angular Resolution

The expected angular resolutions for the K band (22 GHz) and the Q band (43 GHz) are about 1.2 mas and about 0.6 mas, respectively. The synthesized beam size strongly depend on  $UV$  coverage, and could be larger than the values mentioned above because the baselines projected on  $UV$  plane become shorter than the distance between antennas.

### 3.4 Sensitivity

When a target source is observed, a noise level  $\sigma_{\text{bl}}$  for each baseline can be expressed as

$$\sigma_{\text{bl}} = \frac{2k}{\eta} \frac{\sqrt{T_{\text{sys},1} T_{\text{sys},2}}}{\sqrt{A_{e1} A_{e2}} \sqrt{2B\tau}}, \quad (3)$$

where  $k$  is Boltzmann constant,  $\eta$  is quantization efficiency ( $\sim 0.88$ ),  $T_{\text{sys}}$  is system noise temperature,  $A_e$  is antenna effective aperture area which include aperture efficiency,  $B$  is the bandwidth, and  $\tau$  is on-source integration time. Note that for an integration time beyond 3 min (in the K band), the noise level expected by equation (3) cannot be attained because of the coherence loss due to the atmospheric fluctuation. Thus, for finding fringe within a coherence time, the integration time  $\tau$  cannot be longer than 3 minutes. When a continuum source is observed with the digital filter mode of ‘VERA1’ under moderate weather condition, the noise level estimated by the equation (3) is  $\sigma_{\text{bl}}=23$  mJy, assuming that aperture efficiency  $\eta_A \sim 50\%$ ,  $B = 128$  MHz,  $\tau = 120$  sec, and  $T_{\text{sys}} = 200$  K. Thus the minimum flux which can be detected for each baseline is 160 mJy for  $S/N = 7$ . For VLBI observations, signal-to-noise ratio ( $S/N$ ) of at least 5 and usually 7 is generally required for finding fringes. On the other hand, when a maser source is observed with the ‘VERA7’ mode under above conditions, the noise level is  $\sigma_{\text{bl}}=1.5$  Jy, assuming that  $B = 31.25$  KHz (512 spectral channels with 16 MHz bandwidth) for the VERA7 mode. Thus the minimum detectable flux for each baseline is 10.2 Jy for  $S/N = 7$ . A noise level for each parameter is also expressed as follows,

$$\sigma_{\text{bl}} = 23 \times \left( \frac{T_{\text{sys},1}}{200 \text{ K}} \right)^{1/2} \left( \frac{T_{\text{sys},2}}{200 \text{ K}} \right)^{1/2} \left( \frac{B}{128 \text{ MHz}} \right)^{-1/2} \left( \frac{\tau}{120 \text{ sec}} \right)^{-1/2} \text{ mJy}. \quad (4)$$

On the dual-beam observation, a continuum source or a maser source which is brighter than the above baseline sensitivity should be observed as reference source by one of the two beams. If the users observe a source which is weaker than the above sensitivity limit, it is necessary to carry out long time integration with phase-referencing to brighter sources. After successful phase-referencing, signal-to-noise ratio is improved as  $\propto \sqrt{\tau}$ .

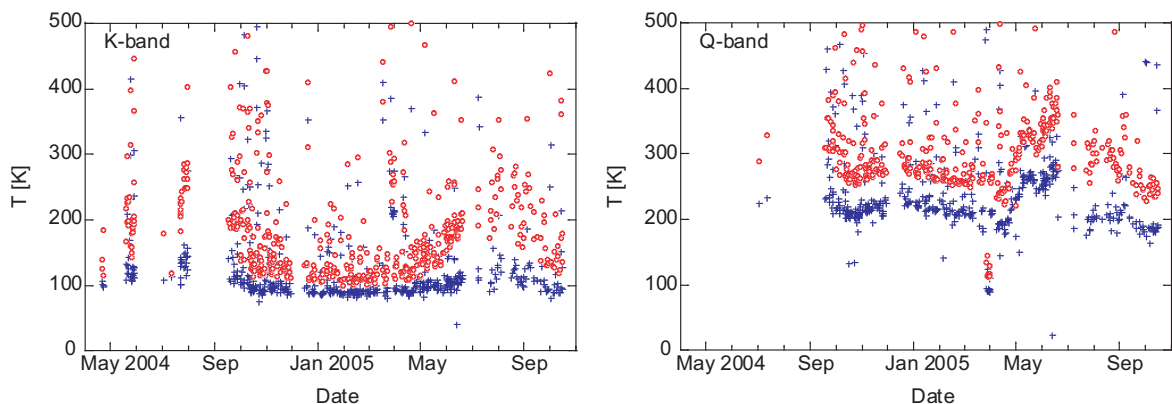


Figure 14: The receiver noise temperature (*blue crosses*) and the system noise temperature (*red open circles*) at the zenith in the K band and the Q band with the Mizusawa antenna.

Figure 14 show the receiver noise temperature and the system noise temperature at the zenith for the K and Q bands, at Mizusawa station. Here the receiver temperature includes the temperature increase due to the feedome loss and the spill-over effect. In Mizusawa, typical system temperature in the K band is  $T_{\text{sys}} = 150$  K in fine weather of winter season, but sometimes rises above  $T_{\text{sys}} = 300$  K in summer season. The system temperature at Iriki station shows a similar tendency to that in Mizusawa. In Ogasawara and Ishigaki-jima, typical system temperature is similar to that for summer in Mizusawa site, with typical optical depth of  $\tau_0 = 0.2 \sim 0.3$ . The typical system temperature in the Q band in Mizusawa is  $T_{\text{sys}} = 250$  K in fine weather of winter season, and  $T_{\text{sys}} = 300 - 400$  K in summer season. The typical system temperature in Ogasawara and Ishigaki-jima in the Q band is larger than that in Mizusawa also.

### 3.5 Astrometric Observation

In an astrometric observation, the observation using dual-beams is recommended. Also, it is strongly recommended to observe pair sources with small separation angle (i.e., less than 1 deg) at high elevation. This will reduce the position errors caused by the residuals in atmospheric zenith delay, which is difficult to predict accurately (e.g., see Reid & Honma 2014). Generally, users are encouraged to carefully carry out data reduction in consultation with a contact person in the VERA project group.

**After the huge earthquake on 11 March 2011, the crustal motion at Mizusawa station is still unstable and may not be simply approximated by linear motion, and this could degrade the astrometric accuracy.**

### 3.6 Calibrator Information

The VLBA calibrator survey of the National Radio Astronomy Observatory (NRAO) is very useful to search for a continuum source which can be used as a reference source to carry out the delay, bandpass, and phase calibrations. The source list of this calibrator survey can be found at the following VLBA homepage,

<http://www.vlba.nrao.edu/astro/calib/index.shtml>.

The calibrator source for phase-referencing should be brighter than the detection limit described in the previous section. For delay calibrations and bandpass calibrations, calibrators with 1 Jy or brighter are recommended.

Regarding H<sub>2</sub>O maser source list, “the Arcetri Catalog of H<sub>2</sub>O maser sources” (Valdettaro et al. 2001, A&A, 368, 845) is very useful. However, we note that the flux of H<sub>2</sub>O maser source is highly variable, and also that it is probable that the correlated flux is significantly lower than that in the catalogued flux because of resolving-out problem with long baselines. We also note that a positional accuracy of a few arcsec is usually needed for correlation process, but some of the maser sources in the catalog have larger position uncertainty.

### 3.7 Nobeyama 45-m and Kashima 34-m Telescopes

The array with the six antennas including Nobeyama 45-m telescope at Nobeyama Radio Observatory (NRO), NAOJ, and Kashima 34-m telescope at Kashima Space



Research Center, National Institute of Information and Communications Technology (NICT), is also available for the K band (22 GHz), but for the Q band (43 GHz) only the Nobeyama 45-m is available in this season. Only a 2-Gbps recording system is available in Nobeyama 45-m and Kashima 34-m.

The observable period for the Nobeyama 45-m telescope is planned to be from December to May, but it may change due to the progress of its maintenance. The Kashima 34-m telescope is not available during its maintenance season usually from August to October. The maintenance season of the Kashima 34-m will change every year. The user can see at the following homepage about the performance of both antennas,

<http://www.nro.nao.ac.jp/~nro45mrt/html/prop/index-e.html>  
<http://www2.nict.go.jp/aeri/sts/stmg/34m/plan/plan34m.html>.

**Both telescopes can not attend to VERA observations in their maintenance period, therefore, the array in which the attendances of the Nobeyama 45-m telescope and/or the Kashima 34-m telescope are essential is unsuitable for a monitoring observation. Whether these antennas are joined in the proposed observation or not is judged by Time Allocating Committee of VERA and NRO based on a scientific merit of observing proposal and availability of observing time.**

Table 10: Performance of Nobeyama 45-m and Kashima 34-m Telescope

Antenna	NRO 45-m		NICT 34-m	
	K band	Q band	K band	Q band
Aperture diameter	45 m		34 m	
Frequency (GHz)	20.0–25.0	42–44	21.8–23.8	42.3–44.9
Beam size (arcsec)	73	39	96	51
Aperture efficiency (%)	66	48	57	20
$T_{\text{sys}}$ (K) <sup>a</sup>	100	150–300	160	350
EL driving range (deg)	12–80		7–88	

<sup>a</sup>Typical system noise temperature in good condition.

### 3.8 Date Archive

The users who proposed the observations will have an exclusive access the data for 18 months after the correlation. After that period, all the observed data in the VERA common-use observation will be released as archive data. Thereafter, archived data will be available to any user upon request. This policy is applied to each observation, even if the proposed observation is comprised of multi-epoch observations in this season.

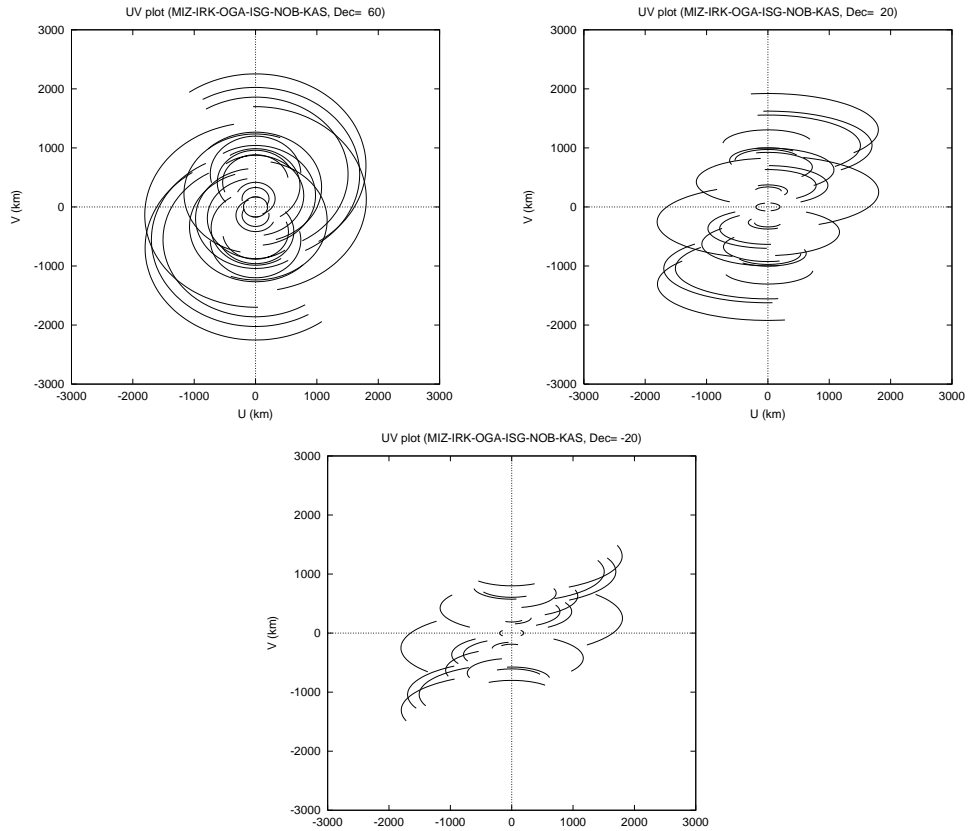


Figure 15:  $UV$  coverage expected with the array of the six antennas, VERA four antennas, NRO 45-m, and NICT 34-m telescopes, from an observation over elevation of  $20^\circ$ . Each panel show  $UV$  coverage for the declination of  $60^\circ$  (*top left*),  $20^\circ$  (*top right*), and  $-20^\circ$  (*bottom*).

## 4 Observation and Data Reduction

### 4.1 Preparation

After the acceptance of proposals, users are requested to prepare the observing schedule file before the observation date. The observer is encouraged to consult a contact person in the VERA project group (which will be assigned after the proposal acceptance) to prepare the schedule file under the support of the contact person.

### 4.2 Observation and correlation

VERA group take full responsibility for observation and correlation process, and thus basically proposers will not be asked to take part in observations or correlations. After the observation and the correlation, the correlated data can be downloaded through an internet in the FITS format. Because the raw data will be erased within 2 months after the correlation, the user should contact the VERA group member within that period if the user needs re-correlation or correlation under different settings (e.g., with different tracking position).

### 4.3 Data Reduction

At present, the users are encouraged to reduce the data using the AIPS. The observation data and calibration data will be provided to the users in a format which AIPS can read.

- As for the amplitude calibration, the VERA's correlation data in FITS format have the system temperature measured by the R-sky method and the information (gain-curve table) of the dependence of aperture efficiency on antenna elevation and separation of dual-beam. If the user wants a weather information, the informations of the temperature, pressure, and humidity during the observation can be provided.
- The calibration data for the dual-beam instrumental phase is provided to the users as text file which can be read as the SN table of AIPS. This text file can be imported using the task "TBIN" of AIPS, and its calibration solution (SN) can be used for updating the calibration gain factor (CL) table using the AIPS task "CLCAL".
- A-priori delay calculation at correlation is not accurate enough for astrometric measurements, and this will be corrected for later with delay-recalculation tools that have higher precision. Basically these corrections will be made before the data are sent to proposers. Please ask a contact person in the VERA project group to check the status of delay recalculation in your data when you receive the data.

In case of questions or problems, users are encouraged to ask the contact person in the VERA group for supports. Also, please check the VERA homepage, where the latest information about data reduction will be shown.

## 4.4 Further Information

The users can contact any staff member of the VERA by E-mail (see table 11).

Table 11: Contact Persons

Name	E-mail address	Related Instrument
K. M. Shibata	k.m.shibata@nao.ac.jp	Operation, Schedule management, Antenna site in general
T. Jike	takaaki.jike@nao.ac.jp	Geodetic measurement
T. Hirota	tomoya.hirota@nao.ac.jp	Performance for each antenna
M. Honma	mareki.honma@nao.ac.jp	Phase calibration, Data analysis

Some documents for the VERA, including user guides and proposal application forms, are accessible on the VERA homepage:

<http://veraserver.mtk.nao.ac.jp/index.html>.